The Isoindazole Nucleus as a Donor in Fullerene-Based Dyads. Evidence for Electron Transfer

ARTICLE *in* THE JOURNAL OF ORGANIC CHEMISTRY · MAY 2004

Impact Factor: 4.72 · DOI: 10.1021/jo0499017 · Source: PubMed

JOC Articles

The Isoindazole Nucleus as a Donor in Fullerene-Based Dyads. Evidence for Electron Transfer

Juan L. Delgado, Pilar de la Cruz, Vicente López-Arza, and Fernando Langa*

Facultad de Ciencias del Medio Ambiente, Universidad de Castilla-La Mancha, 45071, Toledo, Spain

David B. Kimball and Michael M. Haley*

Department of Chemistry and the Materials Science Institute, University of Oregon, Eugene, Oregon 97403-1253

Yasuyuki Araki and Osamu Ito*

Institute of Multidisciplinary Research for Advanced Materials, Tohoku University, Katahira, Sendai, Miyagi 980-8577, Japan

fernando.lpuente@uclm.es

Received January 16, 2004

A series of isoindazole-C_{60} dyads **4a**−**c** based on pyrazolino[60]fullerene have been prepared by 1,3-dipolar cycloadditions of the nitrile imines, generated in situ from hydrazones **3a**−**c**, to C_{60}. Molecular orbital calculations for **4b** revealed that the electron distribution of the HOMO is located on the isoindazole moiety, while the electron distribution of the LUMO is located on the C_{60} moiety. Electrochemical properties of the new dyads **4a**−**c** show a similar electron affinity with respect to C_{60}. Charge-transfer interactions in the ground state between the isoindazole ring and the fullerene cage are predicted by the molecular orbital calculations and confirmed by electrochemical studies in **4a**,**b**. Steady-state fluorescence emission spectra of dyads **4a**−**c** show that fluorescence intensities in polar benzonitrile solvent decrease with increasing electron-donating ability of the substituent attached on the isoindazole group. This was confirmed by the shortening of fluorescence lifetimes, from which intramolecular charge-separation rates and efficiencies via the excited singlet states of the fullerene moiety were evaluated. The yields of the triplet states in polar solvent decrease with the electron-donating ability, supporting the competitive formation of the charge-separated state with the intersystem crossing from the excited states. Thus, isoindazole[60]fullerene **4b** can be considered a molecular switch with an AND logic gate.

Introduction

During the past five years, electron donor−acceptor (DA) dyads based on [60]fullerene, which upon photoexcitation give rise to photoinduced charge-separated states, have been the focus of intensive research as candidates for artificial photosynthetic reaction centers.[1,2] A wide variety of donor fragments such as porphyrin,[3] tetrathiafulvalene,[4] ferrocene,[5] and amines[6] have been used both in the search for improved electron-transfer (ET) properties and to further the understanding of the process. Although derivatization of C_{60} decreases, in general, the electron affinity of the all-carbon sphere as a consequence of the loss of conjugation,[7] we have shown that pyrazolino-[60]fullerenes present an improved electron affinity

(1) Bracher, P. J.; Schuster, D. I. Electron Transfer in Functionalized Fullerenes. In *Fullerenes: From Synthesis to Optoelectronic Properties*; Guldi, D. M., Martin, N., Eds.; Kluwer Academic Publishers: Norwell, MA, 2002; Chapter 6.

(2) (a) Imahori, H.; Sakata, Y. *Adv. Mater.* **1997**, *9*, 537−546. (b) Martín, N.; Sánchez, L.; Illescas, B.; Pérez. I. *Chem. Rev.* **1998**, *98*, 2527−2548. (c) Imahori, H.; Sakata, Y. *Eur. J. Org. Chem.* **1999**, 2445−2457. (d) Guldi, D. M. *Chem. Commun.* **2000**, 321−327. (e) Guldi, D. M.; Prato, M. *Acc. Chem. Res.* **2000**, *33*, 695−703. (f) Nierengarten, J. F.; Armaroli, N.; Accorsi, G.; Rio, Y.; Eckert, J. F. *Chem. Eur. J.* **2003**, *9*, 37−41.

(3) (a) Gust, D.; Moore, T. H.; Moore, A. L. *Acc. Chem. Res.* **2001**, *34*, 40−48. (b) Guldi, D. M. *Chem. Soc. Rev.* **2002**, *31*, 22−36. (c) Liddell, P. A.; Kodis, G.; Moore, A. L.; Moore, T. A.; Gust, D. *J. Am. Chem. Soc.* **2002**, *124*, 7668−7669. (d) Wilson, S. R.; MacMahon, S.; Tat, F. T.; Jarowski, P. D.; Schuster, D. I. *Chem. Commun.* **2003**, 226−227.

(4) (a) Llacay, J.; Veciana, J.; Gancedo, J. V.; Bourdelande, J. L.; Moreno, R. G.; Rovira, C. *J. Org. Chem.* **1998**, *63*, 5201−5210. (b) Pérez, I.; Liu, S.; Martín, N.; Echegoyen, L. *J. Org. Chem.* **2000**, *65*, 3796−3803. (c) Segura, J. L.; Priego, E. M.; Martín, N. *Tetrahedron Lett.* **2000**, *41*, 7737−7741.

(5) (a) Guldi, D. M.; Magini, M.; Scorrano, G.; Prato, M. *J. Am. Chem. Soc.* **1997**, *119*, 974−980. (b) D'Souza, F.; Zandler, M. E.; Smith, P. M.; Deviprasad, K. A.; Fujitsuka, M.; Ito, O. *J. Phys. Chem. A* **2002**, *106*, 649−656. (c) Zandler, M. E.; Smith, P. M.; Fujitsuka, M.; Ito, O.; D'Souza, F. *J. Org. Chem.* **2002**, *67*, 9122−9129. (d) Fujitsuka, M.; Tsuboya, N.; Hamasaki, R.; Ito, M.; Onodera, S.; Ito, O.; Yamamoto, Y. *J. Phys. Chem. A* **2003**, *107*, 1452−1458.

10.1021/jo0499017 CCC: $27.50
Published on Web 03/13/2004

SCHEME 1

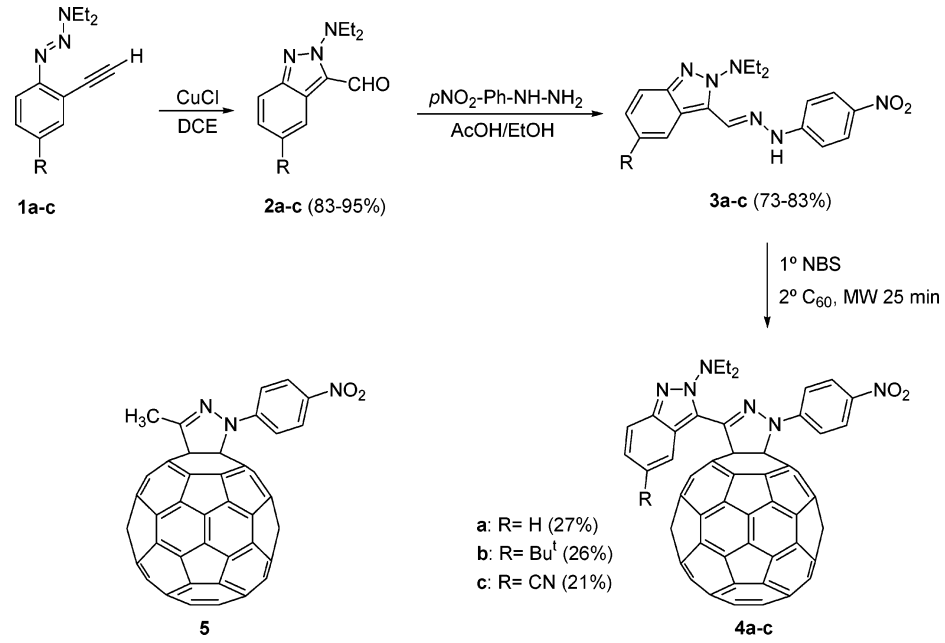

compared to the parent C_{60}[8] (up to 70 mV) because of the inductive effect of the pyrazoline ring. Several DA dyads based on pyrazolino[60]fullerenes have been prepared, and efficient intramolecular photoinduced electron-transfer (PET) processes have been observed.[9] The recent report of an easy, high-yield synthesis of isoindazole aldehydes by heating (2-ethynylphenyl)triazenes with CuCl in 1,2-dichloroethane (DCE)[10] led us to consider this heterocycle as a donor unit in our continuing investigations. Herein, we report the synthesis, theoretical calculations, and the electrochemical and photophysical properties of a series of pyrazolino[60]fullerene dyads in which a 2-aminoisoindazolyl moiety is acting as a donor.

Results and Discussion

Synthesis and Characterization. The synthetic approach to preparing isoindazolylpyrazolino[60]fullerenes **4a**−**c** (Scheme 1) relies upon the 1,3-dipolar cycloaddition of isoindazolyl nitrile imines under microwave irradiation,[11] which in turn can be generated in situ from the corresponding hydrazones **3a**−**c**. This methodology has proven to be a powerful tool for the functionalization of C_{60} due to the availability of the starting materials and the fact that no stereogenic centers are produced during the reaction.[9a] Isoindazole aldehydes **2a**−**c** were prepared by Cu-promoted cyclization of **1a**−**c** as previously described.[10c] Reaction of **2a**−**c** with 4-nitrophenylhydrazine in EtOH under reflux for 10 min afforded hydrazones **3a**−**c** in very good yields (73−83%). Reaction of **3a**−**c** with NBS in $CHCl_3$ at room temperature and subsequent addition of C_{60} and Et_3N in toluene and irradiation in a focused microwave reactor at 210 W for 25 min afforded cycloadducts **4a**−**c** in 21−27% isolated yield after column chromatography (silica gel, toluene) followed by centrifugation in hexane, MeOH, and Et_2O. Cycloadduct **5**, used as a reference, was prepared by a similar procedure from acetaldehyde 4-nitrophenylhydrazone (**6**) and C_{60} in 42% yield.

The structures of hydrazones **3a**−**c**, cycloadducts **4a**−**c** and the reference compound **5** were confirmed by analytical and spectroscopic data. The ^{1}H NMR spectra of **4a**−**c** and **5** in $CDCl_3$ exhibit all of the expected signals corresponding to the organic addendum. The observed signals in the ^{13}C NMR spectra are in agreement with the proposed structures showing the signals originating from the isoindazole moiety as well as most of those from the fullerene system with the appearance of the sp^3 carbons of the C_{60} cage in the range of 82−91 ppm. The structures of **4a**−**c** and **5** were also confirmed by MALDI-TOF mass spectra, which show the expected MH^+ peaks at m/z = 1071 (**4a**), 1127 (**4b**), 1096 (**4c**), and 898 (**5**), together with several fragmentation peaks. Accurate masses of **4a**−**c** (FAB+ technique, see Experimental Section) confirmed the proposed structure.

Molecular Orbital Calculations. The geometries of dyads **4a**−**c** were optimized by semiempirical AM1

(6) (a) Williams, R. M.; Zwier, J. M.; Verhoeven, J. W. *J. Am. Chem. Soc.* **1995**, *117*, 4093−4099. (b) Sun, Y. P.; Ma, B.; Bunker, C. E. *J. Phys. Chem.* **1998**, *102*, 7580−7590. (c) Liu, S. G.; Shu, L.; Raimundo, J. M.; Roncali, J.; Gorgues, A.; Echegoyen, L. *J. Org. Chem.* **1999**, *64*, 4884−4886. (d) Guldi, D. M.; Swartz, A.; Luo, C.; Gómez, R.; Segura, J. L.; Martín, N. *J. Am. Chem. Soc.* **2002**, *124*, 10875−10886.

(7) Echegoyen, L.; Echegoyen, L. E. *Acc. Chem. Res.* **1998**, *31*, 593−601.

(8) Langa, F.; de la Cruz, P.; Espíldora, E.; de la Hoz, A.; Bourdelande, J. L.; Sánchez, L.; Martín. N. *J. Org. Chem.* **2001**, *66*, 5033−5041.

(9) (a) Langa, F.; Gómez-Escalonilla, M. J.; Diez-Barra, E.; García-Martínez, J. C.; de la Hoz, A.; Rodríguez-López, J.; González-Cortés, A.; López-Arza, V. *Tetrahedron Lett.* **2001**, *42*, 3435−3438. (b) Langa, F.; de la Cruz, P.; Delgado, J. L.; Gómez-Escalonilla, M. J.; González-Cortés, A.; de la Hoz, A.; López-Arza, V. *New. J. Chem.* **2002**, *26*, 76−80. (c) Espíldora, E.; Delgado, J. L.; de la Cruz, P.; de la Hoz, A.; López-Arza, V.; Langa F. *Tetrahedron* **2002**, *58*, 5821−5826.

(10) (a) Kimball, D. B.; Hayes, A. G.; Haley, M. M. *Org. Lett.* **2000**, *2*, 3825−3827. (b) Kimball, D. B.; Herges, R.; Haley, M. M. *J. Am. Chem. Soc.* **2002**, *124*, 1572−1573. (c) Kimball, D. B.; Weakley, T. J. R.; Haley, M. M. *J. Org. Chem.* **2002**, *67*, 6395−6405. (d) Kimball, D. B.; Weakley, T. J. R.; Herges, R.; Haley, M. M. *J. Am. Chem. Soc.* **2002**, *124*, 13463−13473.

(11) de la Cruz, P.; Díaz-Ortiz, A.; García, J. J.; Gómez-Escalonilla, M. J.; de la Hoz, A.; Langa, F. *Tetrahedron Lett.* **1999**, *40*, 1587−1590.

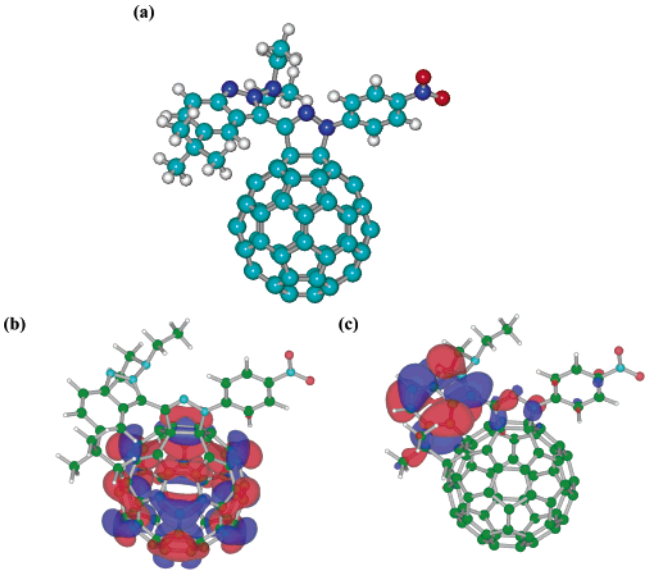

FIGURE 1. (a) Optimized structure, (b) LUMO, and (c) HOMO of **4b** calculated by Gaussian03 at the HF/6-31G level.

calculations. Figure 1 shows the most stable conformation of cycloadduct **4b**. The isoindazole ring is twisted by 50.1° with respect to the pyrazoline ring, whereas the *p*-nitrophenyl group is twisted by 25.3°. The calculated distance between the closest C-atom of the isoindazole ring and the C_{60} surface is 3.27 Å, shorter than the van der Waals radii for C−C interaction (3.40 Å),[12] suggesting that through-space electronic interaction can take place between both moieties.

The electron distributions were calculated by Gaussian 03 at the HF/6-31G level. The electron distributions of the HOMOs of dyads **4a**−**c** are localized on the isoindazole moiety, and the energy levels (**4a**, −8.66 eV; **4b**, −8.56 eV; **4c**, −8.95 eV) are higher in energy relative to pure C_{60} (−9.48 eV). An example of the HOMO is shown in Figure 1c for **4b**. The LUMOs are located in the fullerene cage. An example of the LUMO is shown in Figure 1b for **4b**. The LUMO energy levels of these systems (**4a**, −3.05 eV; **4b**, −3.04 eV; **4c**, −3.10 eV) are lower than that of C_{60} (−2.88 eV). Consequently, these systems present a small HOMO−LUMO gap (**4a**, 5.61 eV; **4b**, 5.52 eV; **4c**, 5.85 eV) enabling intramolecular electron-transfer processes, particularly in the case of **4a**,**b**.

Electrochemistry. The electrochemical behavior of hydrazones **3a**−**c** and dyads **4a**−**c** was studied using cyclic voltammetry (CV) and Osteryoung square-wave voltammetry (OSWV) techniques at room temperature in ODCB/CH_3CN (4:1) as a solvent and using $Bu_4N^+ClO_4^-$ (TBAP) as the supporting electrolyte. The redox potentials of **4a**−**c** and **5** are collected in Table 1 (see the plots in Supporting Information) and compared with those of the precursor hydrazones **3a**−**c** and **6** and C_{60} as a reference.

As a general feature on the reduction side, dyads **4a**−**c** give rise to six one-electron reduction waves. Four of them (E^1_{red}, E^2_{red}, E^4_{red}, and E^6_{red}) are quasi-reversible, corresponding to the fullerene core, while the other two

(12) Bondi, A. J. *J. Phys. Chem.* **1964**, *68*, 441−451.

TABLE 1. Redox Potentials (OSWV) of Organofullerenes 4a−c and 5, Hydrazones 3a−c, 6, and C_{60}[a]

R	E^1_{red}	E^2_{red}	E^3_{red}	E^4_{red}	E^5_{red}	E^6_{red}	E^1_{ox}	E^2_{ox}
4a	−0.63	−1.04	−1.45[b]	−1.59	−1.80 [b]	−1.99	0.87[c]	
4b	−0.63	−1.04	−1.46[b]	−1.59	−1.80[b]	−2.00	0.87[c]	
4c	−0.61	−1.03	−1.44[b]	−1.58	−1.76[b]	−1.99	0.86[c]	
C_{60}	−0.64	−1.05		−1.51		−1.96		
3a			−1.36[b]		−1.81[b]		0.79[c]	1.18[c]
3b			−1.38[b]		−1.82[b]		0.75[c]	1.25[c]
3c			−1.32[b]		−1.73[b]		0.87[c]	1.36[c]
5	−0.63	−1.04	−1.45[b]	−1.64		−1.97		
6			−1.44[b]					1.22[c]

[a] V vs $Ag/AgNO_3$; GCE as the working electrode; 0.1 M TBAP; ODCB/MeCN (4:1); scan rate = 100 mV/s. [b] Irreversible according to CV. [c] Measured by CV.

irreversible CV peaks such as E^3_{red} are assigned to the *p*-nitrophenyl moiety and E^5_{red} to the isoindazole group by comparison with those of the starting hydrazones **3a**−**c**. Similar to other pyrazolino[60]fullerene derivatives,[8,9] the first reduction potentials (E^1_{red}) are analogous to that of pure C_{60} and shifted to more positive values in comparison to other fullerene derivatives due to the $-I$ effect of the pyrazoline ring. The first reduction potential is more shifted toward a positive value in **4c** (30 mV with respect to C_{60}) as a consequence of the presence of the electron-withdrawing cyano group.

On the oxidation side, dyads **4a**−**c** present remarkable donor strength, as a one-electron irreversible wave was observed at around +0.87 V. Hydrazones **3a**−**c** show two oxidation potentials at around 0.8 and 1.2 V (see Table 1). The first one can be assigned to the isoindazole group, and E^2_{ox} must be due to the hydrazone moiety by comparison with the oxidation potential of the hydrazone **6**. When the oxidation potentials of **4a**−**c** are compared with those in hydrazones **3a**−**c** (see Table 1), the potential values of **4a** and **4b** are anodically shifted relative to the corresponding hydrazones **3a** and **3b** by 80 and 120 mV, respectively. This indicates that some degree of charge-transfer exists in the ground state in **4a** and **4b** from the donating isoindazole moiety to the acceptor C_{60} as the molecular orbital calculations predicted. Since this shift is not observed in **4c** as a consequence of the electron-withdrawing effect of the cyano group, it can be concluded that this compound does not show charge-transfer interactions.

UV−Vis Spectra. UV−vis spectra in toluene and benzonitrile of dyads **4a**−**c** are shown in Figure 2. The absorption peaks appearing at 690, 600, 550, and 470−490 nm in the inset of Figure 2 are characteristic of the fullerene moieties.

With changing the isoindazole moieties and solvents, the absorption intensities and peak position varied appreciably. In the region of wavelengths shorter than 430 nm, the main peaks were observed at 330 nm with a shoulder at 380−400 nm. In this region, the absorption of the fullerene moieties and the isoindazole moieties may be overlapped. In addition, the typical absorption band of 1,1-dihydrofullerenes was observed at 426 nm. In nonpolar toluene, shoulders appeared at 400 nm, while this shoulder shifted to a shorter wavelength in polar benzonitrile.

Interestingly, when the spectrum of **4a** was recorded in CH_2Cl_2 (Figure 3), a broad band between 340 and 450 nm appears in comparison with the spectrum in toluene,

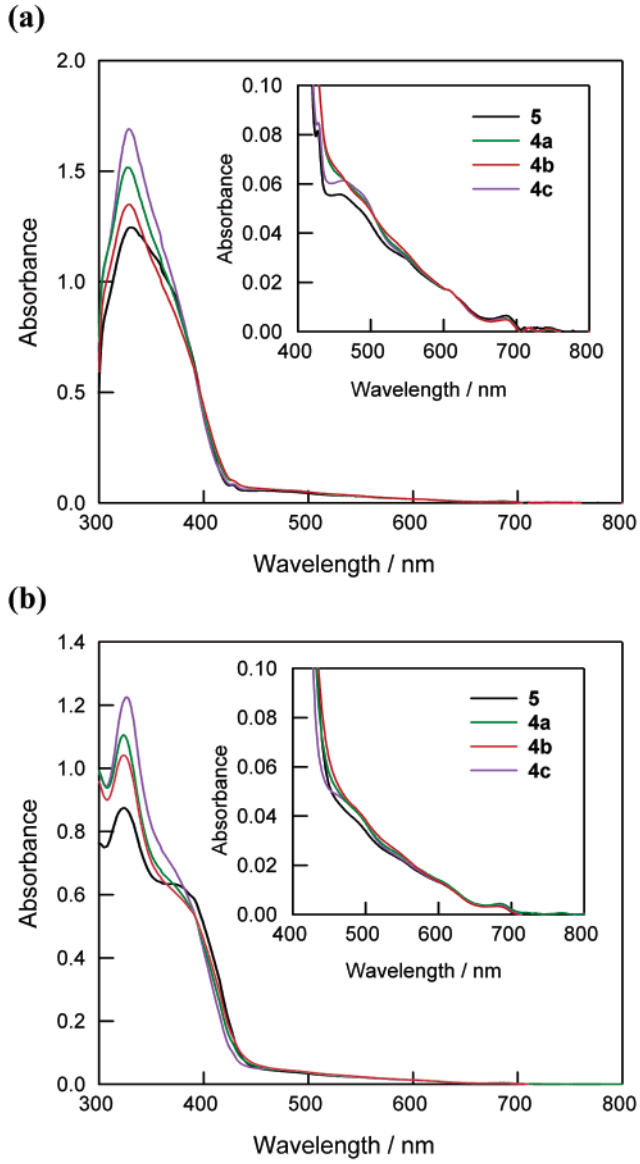

FIGURE 2. Absorption spectra of **4a**−**c** and **5** (0.1 mM) in (a) benzonitrile and (b) toluene. Inset: Enlarged illustration of absorbance.

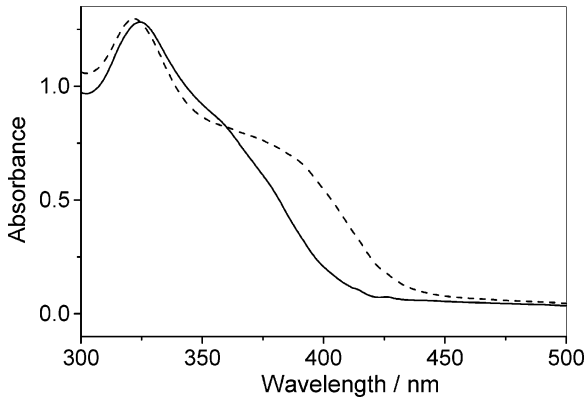

FIGURE 3. UV−vis spectra of **4a** (0.1 mM) in cyclohexane (−) and dichloromethane (- - -).

which revealed some interactions in the ground state[13] between the isoindazole group and the C_{60} cage in polar solvents such as CH_2Cl_2, as suggested by electrochemical studies (vide supra) in more polar solvents.

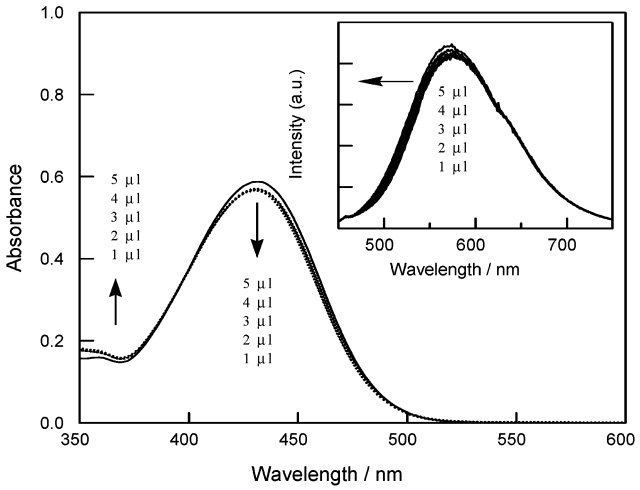

FIGURE 4. Absorption spectra of hydrazone **3b** (0.1 mM) and addition effect of trifluoroacetic acid in benzonitrile. Inset: Fluorescence spectra of **3b** (0.1 mM) (λ_{exc}: 310 nm).

For **3b**, the absorption spectra are shown in Figure 4, in which the peak was observed at 435 nm. However, the corresponding absorption bands were not appreciably observed as shown in Figures 2 and 3. This observation suggests that the hydrazones **3a**−**c** have quite different electronic properties from the isoindazole group attached to the C_{60} cage. On addition of trifluoroacetic acid (TFA) to the hydrazones **3a**−**c** in toluene, appreciable change was not observed in the absorption intensity, peak, and shape as shown in Figure 4. This finding suggests that the hydrazones **3a**−**c** do not have the ability to accept a proton from TFA in toluene.

Steady-State Fluorescence Spectra. The room-temperature fluorescence spectra of hydrazone **3b** in benzonitrile are shown in the inset of Figure 4, in which the fluorescence peak was observed at 580 nm. On addition of TFA in benzonitrile, the fluorescence peak and shape were not changed appreciably. Selected data are summarized in Table 2. In toluene, on the other hand, an appreciable increase in the fluorescence intensity of **3b** was observed.

Fluorescence spectra of the dyads **4a**−**c** and the model *N*-methylpyrrolidino[60]fullerene **5**[14] as a reference were measured in toluene and benzonitrile as shown in Figures 5a and 5b, respectively. In toluene, peaks appeared at 697 nm due to the fullerene moiety.[15]

Since the fluoresence in the 500−600 nm region was not observed for **4a**−**c**, energy transfer takes place efficiently from the excited singlet state of the isoindazole

(13) (a) Nakamura, Y.; Minowa, T.; Tobita, S.; Shizuka, H.; Nishimura. J. *J. Chem. Soc., Perkin Trans. 2* **1995**, 2351−2357. (b) Guldi, D. M.; Maggini, M.; Scorrano, G.; Prato, M. *J. Am. Chem. Soc.* **1997**, *119*, 974−980. (c) Llacay, J.; Veciana, J.; Gancedo, J. V.; Bourdelande, J. L.; Moreno, R. G.; Rovira, C. *J. Org. Chem.* **1998**, *63*, 5201−5210. (d) Fong, R., II; Schuster, D. I.; Wilson, S. R. *Org. Lett.* **1999**, *1*, 729−732. (e) Liu, S. G.; Shu, L.; Rivera, J.; Liu, H.; Raimundo, J. M.; Roncali, J.; Gorgues, A.; Echegoyen, L. *J. Org. Chem.* **1999**, *64*, 4884−4886. (f) Ohno, T.; Moriwaki, K.; Minaya, T. *J. Org. Chem.* **2001**, *66*, 3397−3401.

(14) Maggini, M.; Scorrano, G.; Prato, M. *J. Am. Chem. Soc.* **1993**, *115*, 9798−9799.

(15) At this wavelength, both the isoindazole and the fullerene moieties should be excited according to the UV−vis spectra.

TABLE 2. Fluorescence Peak (λ_F) and Intensity of Compounds 3a−c, 4a−c, and 5

	λ_F (nm)/intensity (a.u.)	
compd[a]	toluene	benzonitrile
3a	565/43	
3b	565/45	
3c	570/42	
4a	697/110	697/62
4b	967/110	697/100
4c	699/108	697/38
5	699/112	697/114

[a] λ_{exc} = 400 nm in toluene and benzonitrile at the same absorbance.

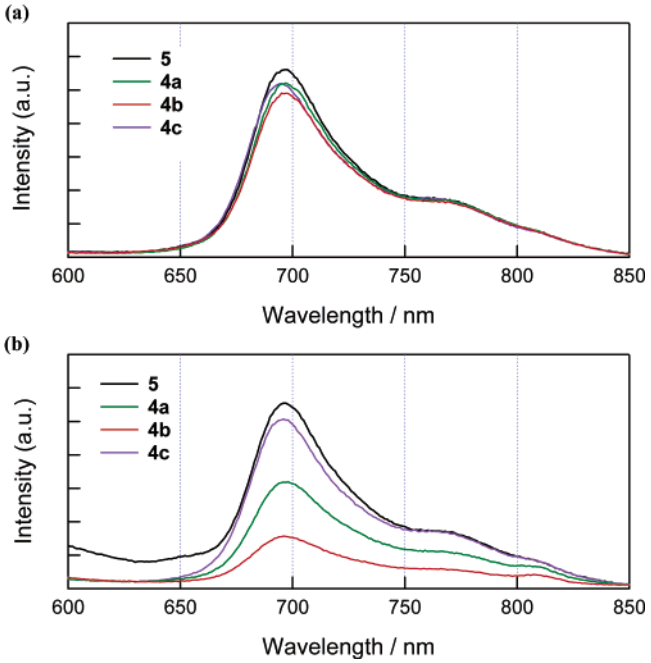

FIGURE 5. Fluorescence spectra of dyad **4a−c** and **5** in (a) toluene and (b) in benzonitrile; λ_{exc} = 400 nm.

(or hydrazone) moiety to the fullerene moieties, which exhibit peaks at 697 nm. In toluene, an appreciable substituent effect was not observed among **4a−c**. In benzonitrile, on the other hand, the fluorescence intensities at 697 nm of the fullerene moieties vary considerably from reference **5** and **4c** to **4a** and **4b** (Figure 5b). With increasing electron-donating ability of the substituents of the isoindazole moiety, the fluorescence intensity decreased significantly.

Time Profiles of Fluorescence Measurements. Time profiles of fluorescence intensities were measured for reference **5** and **4a−c** in benzonitrile as shown in Figure 6. Fluorescence decay of **4c** is as slow as that of reference **5**, while the fluorescence decay rates increase for **4a** and **4c**, suggesting that quenching occurs via the excited singlet states of fullerene moieties. These observations are in good agreement with the fluorescence intensities. In toluene, the fluorescence time profiles are all the same among **4a−c** and **5**, suggesting that nothing occurs via the excited singlet state of the fullerenes in toluene. All of these fluorescence time profiles are curve-fitted with a single-exponential function, giving the lifetimes (τ_F) as summarized in Table 3. From these τ_F values, the quenching rate constants (k_q) and quantum yields (Φ_q) were calculated as listed in Table 3.

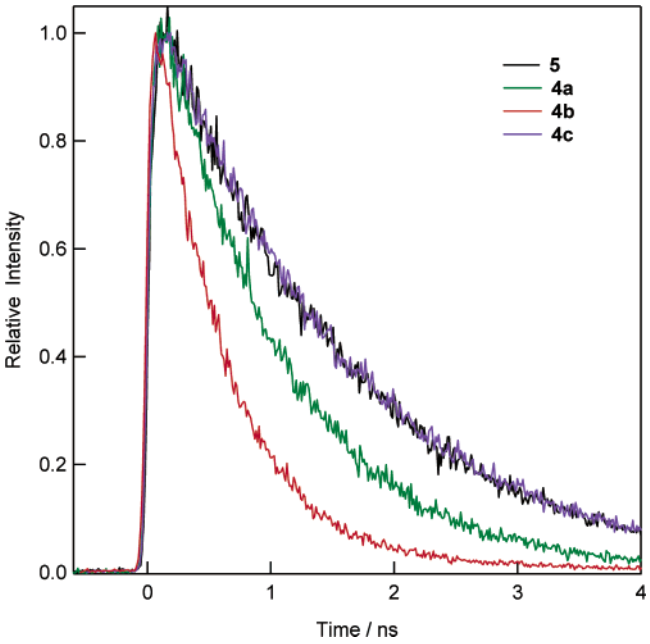

FIGURE 6. Fluorescence time profiles of **4a−c** and **5** in benzonitrile; λ_{exc} = 400 nm.

TABLE 3. Fluorescence Lifetimes (τ_F), Quenching Rate Constants (k_q), Quenching Quantum Yields (Φ_q), and Free-Energy Changes for Charge Separation (ΔG_{CS}) of Compounds 4a−c and 5

compd	solvent	τ_f (ns)[a]	k_q (s^{-1})[b]	Φ_q	ΔG_{CS} (eV)[c]
4a	toluene	1.51	8.7×10^6	0.01	
4a	PhCN	0.98	3.5×10^8	0.35	−0.36
4b	toluene	1.46	3.1×10^7	0.05	
4b	PhCN	0.59	1.0×10^9	0.60	−0.36
4c	toluene	1.46	3.1×10^7	0.05	
4c	PhCN	1.33	8.5×10^7	0.11	−0.39
5	toluene	1.53			
5	PhCN	1.50			

[a] λ_{exc} = 400 nm in toluene and benzonitrile at the same absorbance. [b] Calculated by the following equations; $k_q^S = \tau_F^{-1} - \tau_0^{-1}$ and $\Phi_q^S = (\tau_F^{-1} - \tau_0^{-1})/\tau_F^{-1}$, where lifetimes of references (**5**) are referred to τ_0. [c] ΔG_{CS}^S values were calculated from the Weller equation ($\Delta G_{CS} = E_{ox}$ (TPA) $- E_{red}(C_{60}) - E_0 - E_c$),[34] employing the E_S energy level of $^1C_{60}$* (1.75 eV), the $E_{red}(C_{60})$, and the E_{ox} (**4a−c**) shown in Table 1.

Since the k_q and Φ_q values increase with the electron-donating substituents of the isoindazole moiety in polar solvents, we can conclude that the intramolecular charge separation takes place via the excited singlet state of fullerenes; thus, the k_q and Φ_q values can be put equal to the k_{CS} and Φ_{CS} values in benzonitrile, which can be supported by the electron distribution of HOMO and LUMO in Figures 1b and 1c. The charge separation generates the radical cation in the isoindazole moiety as supposed by the hole distribution in the HOMO, while the radical anion is generated on the C_{60} moiety as the electron distribution of the LUMO.

Transient Absorption Measurements. To confirm the charge-separation state, we employed nanosecond transient absorption spectra, because the k_{CS} values are on the nanosecond time scale. The observed transient spectra for **4a−c** and **5** in benzonitrile are shown in

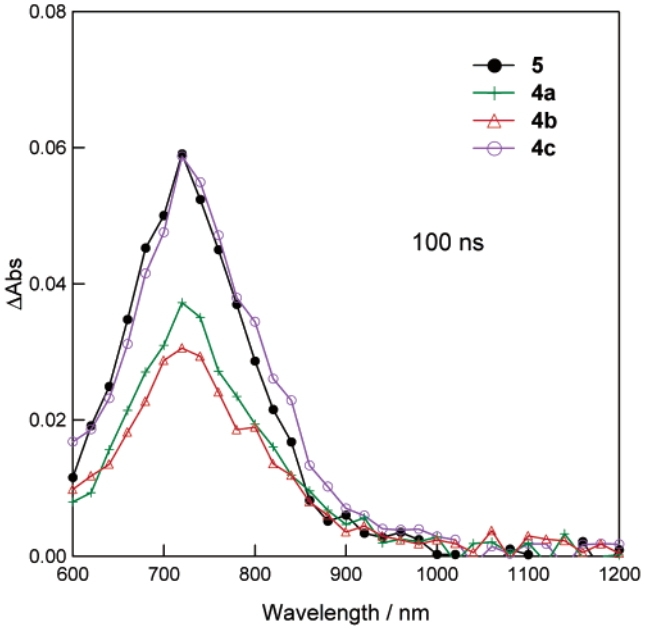

FIGURE 7. Nanosecond transient absorption spectra observed by the 532 nm laser light excitation of **4a**−**c** and **5** in deaerated benzonitrile.

TABLE 4. T−T Absorption Peak (λ_T), Quantum Yields (Φ_T), and Free-Energy Changes for Charge Recombination (ΔG_{CR}) of Compounds 4a−c and 5

compd[a]	solvent	λ_T (nm)	Φ_T	ΔG_{CR} (eV)
4a	toluene	720	0.92	
4a	PhCN	720	0.57	−1.42
4b	toluene	720	0.92	
4b	PhCN	720	0.47	−1.42
4c	toluene	720	0.92	
4c	PhCN	720	0.90	−1.39
5	toluene	720	0.92	0
5	PhCN	720	0.90	0

[a] λ_{exc} = 532 nm in toluene and benzonitrile.

Figure 7. A similar transient absorption band was observed centered at 720 nm for **4a**−**c** and **5**; the 720 nm band was attributed to the triplet excited state of the fullerene moieties. However, the intensity of the 720 nm peak in benzonitrile decreases in the order of electron-donating ability of the substituents on the isoindazole moiety, which implies that the decreased amount of the triplet state is consumed at the excited singlet state as the charge separation before coming to the triplet state via intersystem crossing. The quantum yields (Φ_T) are listed in Table 4, which can have tendencies opposite to the Φ_{CS} values via the excited singlet state of the fullerene moiety.

These observed phenomena can be reasonably explained by energy diagrams as shown in Figure 8, in which the charge separation via the excited singlet state is a competitive process with the intersystem crossing with high quantum yields. The quantum yield for the triplet formation (Φ_T) can be represented by the ratio of $k_{isc}/(k_{cs} + k_{ics})$. From Tables 3 and 4, this relation is satisfied. In toluene, the CS state becomes unstable, lying higher than the excited singlet state of the fullerene; thus, the CS process does not take place, but the ISC to the triplet state predominates.

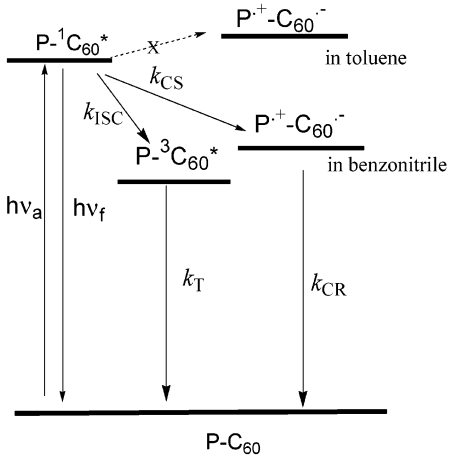

FIGURE 8. Schematic energy diagrams.

Acid Addition Effect. Addition of increasing amounts of TFA to a benzonitrile solution of **4b** causes no change in the absorption spectra, as shown in Figure 9a in the region of wavelengths longer than 400 nm. In the fluorescence spectra shown in Figure 9b, an appreciable change occurs in the fluorescence spectrum in the 650−850 nm region due to the fluorescence of the C_{60} cage, which is in good agreement with the absence of change in the absorption spectra. On the other hand, the fluorescence peak observed at 435 nm in the absence of TFA increased its intensity with a blue shift. The origin of the 435 nm fluorescence peak may be the isoindazole moiety, although the fluorescence peak shifted from the corresponding hydrazone **3b** probably because of the addition to the C_{60} cage. Besides such fluorescence changes with addition of TFA, no change was observed in the fluorescence peak of the C_{60} cage, which suggests that the donor ability of the isoindazole moiety does not decrease due to the protonation of the isoindazole moiety.

The observed appreciable recovery of the fluorescence in 350−450 nm (Figure 9b) can be utilized as an AND logic gate (Figure 10) for this compound.[18] Only fluorescence at 380 nm (switching ON) can be observed when both inputs are 1 (in the presence of irradiation and TFA addition); when one of either inputs is 0, the molecular switch is OFF.

Conclusion

In summary, we have synthesized a novel series of isoindazole-C_{60} dyads **4a**−**c** that show an improved electron affinity with respect to other fullerene derivatives. Good agreement is found between theoretical calculations and electrochemical studies of charge-transfer interactions in the ground state between the isoindazole ring in **4a**,**b**. Steady-state fluorescence emission spectra and fluorescence lifetimes of dyads **4a**−**c**

(16) Solutions with the same absorbance were employed so that the fluorescence and the quantum yields could be correlated.

(17) Armaroli, N. Photoinduced Energy Transfer Processes in Functionalized Fullerenes. In *Fullerenes: From Synthesis to Optoelectronic Properties;* Guldi, D. M., Martin, N., Eds.; Kluwer Academic Publishers: Norwell, MA, 2002; Chapter 5.

(18) Prasanna de Silva, A.; McClenaghan, N. D.; McCoy, C. P. Molecular Logic Systems. In *Molecular Switches*; Feringa, B. L., Ed. Wiley-VCH: Weinheim, 2001; Chapter 11.

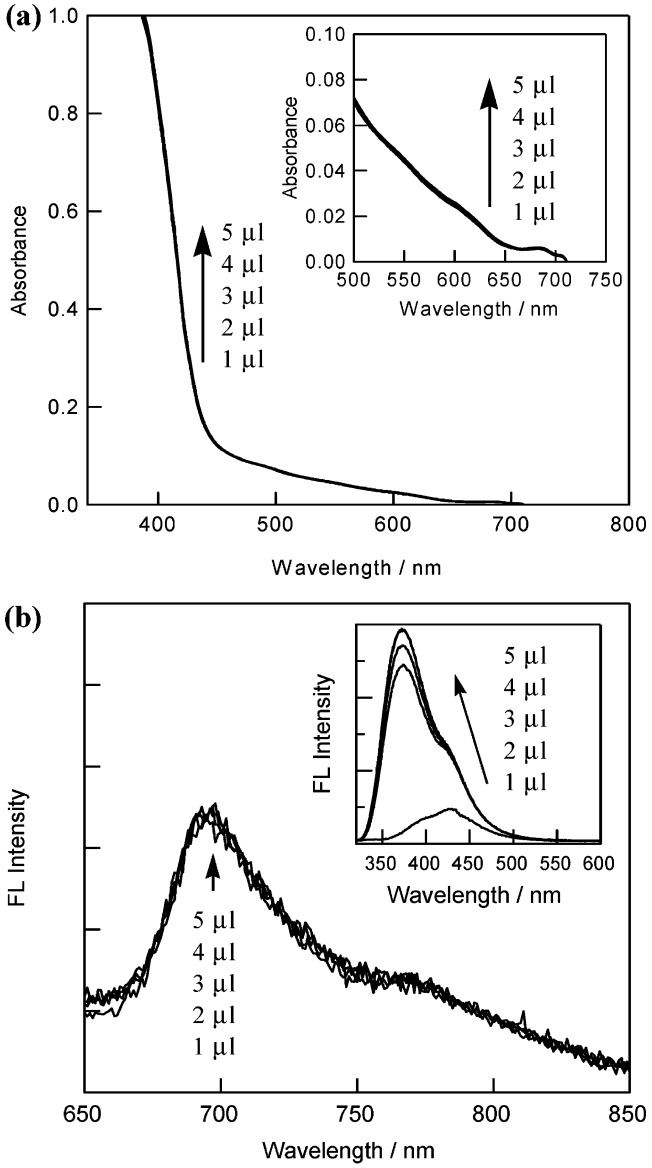

FIGURE 9. (a) Absorption spectra of **4b** (0.1 mM) in benzonitrile and trifluoroacetic acid addition effect. Inset: Enlarged illustration of absorbance in longer wavelngth region. (b) Fluorescence spectra of **4b** (0.1 mM, λ_{exc} = 300 nm) in benzonitrile upon increasing the amount of trifluoroacetic acid. Inset: Fluorescence spectra at shorter wavelengths.

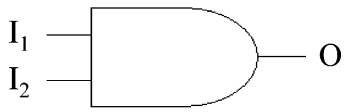

I_1	I_2	O
0	0	0
0	1	0
1	0	0
1	1	1

FIGURE 10. AND logic gate and its corresponding truth table for **4b** (I_1, Irradiation at 430 nm; I_2, addition of TFA; O, fluorescence; 1 = yes, O = no.

show the occurrence of photoinduced electron-transfer processes in benzonitrile. Isoindazole[60]fullerene **4b** can be consider a molecular switch with an AND logic gate.

Experimental Section

2-Diethylamino-2*H*-indazole-3-carboxaldehyde 4-nitrophenylhydrazone (3a): yield 76%; mp 184−186 °C; FT-IR (KBr) ν (cm^{-1}) 3191, 2993, 1586, 1275, 1109, 990, 751, 625; ^{1}H NMR (CD_2Cl_2) δ 0.82 (t, 6H, J = 7.3 Hz), 3.18 (m, 2H), 3.41 (m, 2H), 7.20 (d, 2H, J = 9.5 Hz), 7.26 (dd, 1 H, J = 8.1 Hz, 6.6 Hz), 7.38 (dd, 1H, J = 8.8 Hz, 6.6 Hz), 7.67 (dd, 1H, J = 8.8 Hz), 8.21 (d, 2H, J = 9.5 Hz), 8.26 (d, 1H, J = 8.1 Hz), 8.41 (s, 1H, NH), 8.42 (s, 1H); ^{13}C NMR ($CDCl_3$) δ 11.9, 52.4, 111.7, 117.4, 122.1, 123.4, 126.2, 127.1, 131.3, 132.5, 140.0, 146.3, 149.5; UV−vis (CH_2Cl_2) λ_{max} (nm) (log ϵ) 416.0 (4.8). Anal. Calcd for $C_{18}H_{20}O_2N_6$: C, 61.35; H, 5.72; N, 23.85. Found: C, 60.65; H, 5.45; N, 23.93.

5-*tert*-Butyl-2-diethylamino-2*H*-indazole-3-carboxaldehyde 4-Nitrophenylhydrazone (3b): yield 83%; mp 214−216 °C; FT-IR (KBr) ν (cm^{-1}) 3417, 1494, 1308, 1268, 1103, 831; ^{1}H NMR ($CDCl_3$) δ 0.84 (t, 6H, J = 7.0 Hz), 1.52 (s, 9H), 3.15 (m, 2H), 3.36 (m, 2H), 7.20 (d, 2H, J = 9.1 Hz), 7.53 (dd, 1H, J = 9.1 Hz, 2.2 Hz), 7.69 (d, 1H, J = 9.1 Hz), 8.23 (d, 1H, J = 2.2 Hz), 8.25 (d, 2H, J = 9.1 Hz), 8.27 (s, 1H, NH), 8.40 (s, 1H); ^{13}C NMR ($CDCl_3$) δ 12.0, 31.2, 35.0, 52.4, 111.6, 116.3, 117.2, 117.4, 126.3, 126.7, 131.0, 132.4, 140.3, 145.1, 146.5, 149.4; UV−vis (CH_2Cl_2) λ_{max} (nm) (log ϵ) 419.0 (4.7). Anal. Calcd for $C_{22}H_{28}O_2N_6$: C, 64.68; H, 6.91; N, 20.57. Found: C, 64.10; H, 6.73; N, 19.41.

5-Carbonitrile-2-diethylamino-2*H*-indazole-3-carboxaldehyde 4-Nitrophenylhydrazone (3c): yield 73%; mp 280−282 °C; FT-IR (KBr) ν (cm^{-1}) 3417, 1600, 1481, 1109, 851, 513; ^{1}H NMR (CD_2Cl_2) δ 0.38 (t, 6H, J = 7.0 Hz), 3.20 (m, 2H), 3.39 (m, 2H), 7.22 (d, 2 H, J = 9.5 Hz), 7.51 (d, 1H, J = 8.8 Hz), 7.75 (d, 1H, J = 8.8 Hz), 8.24 (d, 2H, J = 9.5 Hz,), 8.40 (s, 1H), 8.52 (s,1H, NH), 8.68 (s, 1H); ^{13}C NMR (DMSO) δ 7.1, 47.2, 100.6, 107.3, 111.1, 114.5, 115.2, 121.7, 123.2, 124.8, 127.2, 129.0, 134.7, 141.4, 145.0; UV−vis (CH_2Cl_2) λ_{max} (nm) (log ϵ) 416.0 (4.6), 427.5 (4.6). Anal. Calcd for $C_{19}H_{19}O_2N_7$: C, 60.47; H, 5.07; N, 25.98. Found: C, 60.16; H, 5.06; N, 25.63.

3′-(2-Diethylamino-indazolyl)-1′-(4-nitrophenyl)pyrazolino[60]fullerene (4a): yield 27% (62% based on recovered C_{60}); FT-IR (KBr) ν (cm^{-1}) 1587, 1494, 1096, 1043, 871, 838, 738, 519; ^{1}H NMR ($CDCl_3$) δ 1.1 (t, 6H, J = 7.3 Hz), 3.4 (q, 4H, J = 7.3 Hz), 7.13 (dd, 1H, J = 8.2 Hz, 6.6 Hz) 7.3 (dd, 1H, J = 8.8 Hz, 6.6 Hz), 7.6 (d, 1H, J = 8.2 Hz), 7.7 (d, 1H, J = 8.8 Hz), 8.28 (d, 2H, J = 9.2 Hz), 8.37 (d, 2H, J = 9.2 Hz); ^{13}C NMR ($CDCl_3$) δ 12.4, 52.3, 82.8, 89.6, 118.1, 119.1, 120.2, 121.1, 123.3, 124.0, 125.4, 126.4, 135.8, 137.2, 138.4, 139.4, 140.8, 141.9, 142.0, 142.2, 142.3, 142.4, 142.5, 142.9, 142.9, 143.2, 144.0, 144.3, 144.6, 145.1, 145.2, 145.3, 145.4, 145.5, 146.0, 146.1, 146.2, 146.4, 147.2, 147.7, 149.5; UV−vis (CH_2Cl_2) λ_{max} (nm) (log ϵ) 255.0 (5.1), 322.0 (4.8), 387.0 (4.5); MS m/z 1071 (M + 1), 720 (C_{60}). Accurate mass (m/z): 1071.1597 (calcd for $C_{78}H_{19}N_6O_2$: 1071.1569).

3′-(2-Diethylamino-5-*tert*-butyl-indazolyl)-1′-(4-nitrophenyl)pyrazolino[60]fullerene (4b): yield 26% (71% based on recovered C_{60}); FT-IR (KBr) ν (cm^{-1}) 1580, 1474, 1103, 1030, 871, 831, 784, 745, 513; ^{1}H NMR ($CDCl_3$) δ 1.12 (t, 6H, J = 7.3 Hz), 1.28 (s, 9H), 3.44 (q, 4H, J = 7.3 Hz), 7.45 (dd, 1H, J = 9.2 Hz, 1.8 Hz), 7.59 (dd, 1H, J = 1.8 Hz, 1.1 Hz), 7.72 (dd, 1H, J = 9.2 Hz, 1.1 Hz), 8.30 (d, 2H, J = 9.5 Hz), 8.38 (d, 2H, J = 9.5 Hz); ^{13}C NMR ($CDCl_3$) δ 12.3, 31.1, 34.7, 52.4, 83.5, 89.2, 115.0, 117.7, 118.8, 120.6, 123.6, 125.3, 125.8, 135.6, 137.0, 138.1, 139.3, 140.7, 141.8, 141.9, 142.1, 142.2, 142.3, 142.8, 143.1, 143.9, 144.2, 144.5, 144.7, 145.1, 145.2, 145.2, 145.3, 145.4, 145.5, 145.8, 146.0, 146.1, 146.3, 147.0, 147.6, 149.3; UV−vis (CH_2Cl_2) λ_{max} (nm) (log ϵ) 256.0 (5.2), 321.0 (4.8), 394 (3.5); MS m/z: 1127 (M + 1), 720 (C_{60}). Accurate mass (m/z): 1127.2164 (calcd for $C_{82}H_{27}N_6O_2$: 1127.2195).

3′-(2-Diethylamino-5-carbonitrile-indazolyl)-1′-(4-nitrophenyl)pyrazolino[60]fullerene (4c): yield 21% (82% based on recovered C_{60}); FT-IR (KBr) ν (cm^{-1}) 3417, 1600, 1481, 1109, 851, 745, 513; ^{1}H NMR ($CDCl_3$) δ 1.11 (t, 6H, J = 7.3 Hz), 3.42 (q, 4H, J = 7.3 Hz), 7.48 (d, 1H, J = 9.2 Hz), 7.84 (d, 1H, J = 9.2 Hz), 8.18 (s, 1H), 8.25 (d, 2H, J = 9.2 Hz), 8.38 (d,

2H, J = 9.2 Hz); ^{13}C NMR ($CDCl_3$) δ 12.5, 52.7, 83.4, 89.4, 107.1, 119.7, 119.9, 120.6, 125.8, 127.4, 128.3, 128.5, 129.3, 131.2, 136.2, 137.2, 137.4, 139.8, 141.1, 141.8, 142.2, 142.3, 142.4, 142.5, 142.7, 143.3, 143.5, 144.3, 144.6, 144.7, 144.9, 145.5, 145.7, 146.3, 146.4, 146.6, 146.7, 147.5, 149.4; UV−vis (CH_2Cl_2) λ_{max} (nm) (log ϵ) 258.0 (5.3), 321.5 (5.0), 390.0 (4.6); MS m/z 1096 (M + 1), 720 (C_{60}). Accurate mass (m/z): 1096.1513 (calcd for $C_{79}H_{18}N_7O_2$: 1096.1521).

3′-Methyl-1′-(4-nitrophenyl)pyrazolino[60]fullerene (5). An Ar-blanketed solution of NBS (0.10 mmol) and the acetaldehyde 4-nitrophenylhydrazone[21] (0.10 mmol) in dry $CHCl_3$ (30 mL) was stirred at room temperature for 30 min. The solvent was removed in vacuo, and a solution of C_{60} (0.10 mmol) and NEt_3 (0.15 mmol) in dry toluene (50 mL) was added to the solid. The solution was stirred at room temperature for 10 min. The solvent was removed under reduced pressure. The resulting solid was purified by silica gel flash chromatography using toluene as an eluent. Centrifuging three times with MeOH and once with Et_2O accomplished further purification of the solid: yield 42% (60% based on recovered C_{60}); FT-IR (KBr) ν (cm^{-1}) 1593, 1500, 1310, 1231, 1104, 838, 746, 525; ^{1}H NMR ($CDCl_3$) δ 2.87 (s, 3H), 8.18 (d, 2H, J = 9.53 Hz), 8.32 (d, 2H, J = 9.53 Hz); ^{13}C NMR ($CDCl_3$) δ 15.7, 83.7, 88.5, 118.4, 125.5, 136.1, 137.0, 139.2, 141.1, 141.7, 141.9, 142.0, 142.1, 142.3, 142.4, 142.5, 142.9, 143.0, 143.2, 143.7, 144.2, 144.4, 144.6, 145.1, 145.2, 145.3, 145.4, 145.5, 145.9, 146.1, 146.2, 146.3, 146.4, 146.5, 146.6, 147.2, 147.8, 150.2; UV−vis (CH_2Cl_2) λ_{max} (nm) (log ϵ) 229.0 (4.9), 255.0 (5.5), 322.0 (4.5); MS m/z 898.1 (M + 1), 720.0 (C_{60}).

Acknowledgment. Financial support for this work was provided by a grant from Ministerio de Ciencia y Tecnología of Spain and FEDER funds (Project BQU2-001-1512), the Junta de Comunidades de Castilla-La Mancha (Project PAI-02-023), and the National Science Foundation (CHE-0104854). The authors (Y.A. and O.I.) are also grateful for the financial support from Core Research for Evolutional Science and Technology (CREST) of Japan Science and Technology Agency and a Grant-in-Aid for Scientific Research (Nos. 10207202, 11740380, and 12875163).

Supporting Information Available: General remarks, experimental procedures, copies of ^{1}H NMR and ^{13}C NMR spectra, HPLC plots for all compounds, as well as plots of cyclic voltammetries of **4a**−**c**. This material is available free of charge via the Internet at http://pubs.acs.org.

JO0499017

(19) (a) Komamine, S.; Fujitsuka, M.; Ito, O.; Morikawa, K.; Miyata, T.; Ohno, T. *J. Phys. Chem. A* **2000**, *104*, 11497. (b) Fujitsuka, M.; Ito, O.; Yamashiro, T.; Aso, Y.; Otsubo, T. *J. Phys. Chem. A* **2000**, *104*, 4876. (c) Yamazaki, M.; Araki, Y.; Fujitsuka, M.; Ito, O. *J Phys. Chem. A* **2001**, *105*, 8615.

(20) (a) Watanabe, A.; Ito, O.; *J. Phys. Chem.* **1994**, *98*, 7736. (b) Ito, O.; Sasaki, Y.; Yoshikawa, Y.; Watanabe, A. *J. Phys. Chem.* **1995**, *99*, 9838. (c) Alam, M. M.; Watanabe, A.; Ito, O. *Bull. Chem. Soc. Jpn.* **1997**, *70*, 1833.

(21) McElvain, S. M. *The Characterization of Organic Compound*, 3rd ed.; The MacMillan: New York, 1953.